https://doi.org/10.5194/nhess-2019-139
Preprint. Discussion started: 27 May 2019

Natural Hazards and Earth System Sciences
Discussions

Tsunami risk assessment for multiple buildings by considering spatial correlation of wave height using copulas

Yo Fukutani[1], Shuji Moriguchi[2], Kenjiro Terada[2], Takuma Kotani[3], Yu Otake[4], Toshikazu Kitano[5]

[1]College of Science and Engineering, Kanto Gakuin University, Yokohama, 236-8501, Japan
[2]International Research Institute of Disaster Science, Tohoku University, Sendai, 980-8572, Japan
[3]Nippon Koei Co., Ltd, Ibaraki, 300-1259, Japan
[4]Faculty of Engineering, Niigata University, Niigata, 950-2102, Japan
[5]Civil and Environmental Engineering, Nagoya Institute of Technology, Nagoya, 466-8555, Japan

Correspondence to: Yo Fukutani (fukutani@kanto-gakuin.ac.jp)

Abstract. It is necessary to consider simultaneous damage to multiple buildings when performing probabilistic risk assessment for a portfolio of buildings. In this study, we demonstrate tsunami risk assessment for two buildings using copulas of tsunami hazards that consider the nonlinear spatial correlation of tsunami wave heights. First, we simulated the wave heights considering uncertainty by varying the slip amount and fault depths. The frequency distributions of the wave heights were evaluated via the response surface method. Based on the distributions and numerically simulated wave heights, we estimated the optimal copula via maximum likelihood estimation. Subsequently, we evaluated the simultaneous distributions of the wave heights and the aggregate damage probabilities via the marginal distributions and the estimated copulas. As a result, the aggregate damage probability of the ninety-ninth percentile value was approximately 1.0 % higher and the maximum value was approximately 3.0 % higher while considering the wave height correlation. We clearly showed that the usefulness of copula modeling considering the wave height correlation in evaluating risk of building portfolio. We only demonstrated the evaluation method for two buildings, but the effect of the wave height correlation on the results is expected to increase if more points are targeted.

1 Introduction

Probabilistic risk assessment methods of disasters are developed mainly in the field of nuclear safety focused on countermeasures relative to severe accidents at nuclear power plants. Among them, the probabilistic risk assessment method for tsunami disasters was rapidly developed since the 2000s (e.g., Geist and Parsons, 2006; Annaka et al., 2007; González et al., 2009; Thio et al., 2010; Løvholt et al., 2012; Goda et al., 2014; Fukutani et al., 2015; Park and Cox, 2016; De Risi and Goda, 2017). Several extant studies proposed a method of probabilistic risk assessment for an individual site in a local area. Detailed risk assessment for a local area is undoubtedly important in terms of grasping the risk of exposing assets located in the area.

https://doi.org/10.5194/nhess-2019-139
Preprint. Discussion started: 27 May 2019


Natural Hazards and Earth System Sciences Discussions

However, probabilistic evaluation methods are also utilized in cases to evaluate risks for a portfolio of buildings. With respect to businesses that own building portfolios including factories and offices over a wide area, it is extremely important in risk-based management decisions to evaluate the detailed risks posed by aggregates of building portfolios. While evaluating physical risks over a wide area, it is necessary to evaluate the aggregate risk for multiple buildings that are located at a distance. In these types of cases, it is necessary to evaluate the risk by considering the spatial correlation of hazards. Analyses that do not consider the spatial correlation of hazards involves the risk of underestimating the risk over a wide area. Analyses that consider the spatial correlation of hazards are relatively advanced in the field of earthquake risk assessment (e.g., Boore et al., 2003; Wang and Takada, 2005; Park et al., 2007) albeit insufficient in the field of tsunami risk assessment. Analyses that consider the hazard correlation using copulas are used in hydrological/earthquake modeling (e.g., Salvadori et al., 2016; Goda and Tesfamariam, 2015) although there is a paucity of the same in tsunami modeling.

In this study, we assume the occurrence of a large earthquake in the Sagami Trough in Japan that significantly affects the metropolitan area and evaluate the tsunami risk of two buildings located at distant locations by considering the spatial correlation of the tsunami wave height between the two sites. The objective of this study involves evaluating the frequency distribution of the tsunami height via the response surface method and evaluating the spatial correlation of the tsunami height by using various copulas. Specifically, we analyze the frequency distribution (marginal distribution) of tsunami height via the response surface method and target two steel buildings located at Oiso and Miura along the Sagami Bay, Kanagawa Prefecture in Japan. Subsequently, we derive a simultaneous distribution of tsunami wave heights between two sites by using various copula, convert it to the simultaneous distribution of damage via applying a damage function, and evaluate the expected value of the aggregate damage probability for the target buildings. Finally, we confirm the extent to which the expected value of the aggregate damage probability fluctuates in a case where the spatial correlation of tsunami wave height is considered and a case where it is not considered.

The second chapter provides an outline of the response surface method and tsunami risk assessment method for multiple buildings using copulas. The third chapter describes a case where the proposed method is applied to the Sagami trough area. The final conclusions are discussed in the fourth chapter.

2 Methodology

Figure 1 shows a flowchart of tsunami risk assessment considering the correlation of tsunami wave heights in this study. Herein, the risk assessment target points only correspond to two points: Oiso and Miura. First, we simulate the tsunami wave heights considering the uncertainty at the target sites by numerical tsunami simulations via nonlinear long wave equations. Based on this, we construct a response surface and apply probability distributions to obtain a frequency distribution of tsunami wave heights. This distribution becomes a marginal distribution for a joint distribution of tsunami wave heights of two target points. Separately, we estimate appropriate copula via maximum likelihood estimation from the simulation results of the tsunami wave height considering uncertainty. Subsequently, we obtain a joint distribution of tsunami wave heights

https://doi.org/10.5194/nhess-2019-139
Preprint. Discussion started: 27 May 2019


Natural Hazards and Earth System Sciences Discussions

from the estimated copula and the marginal distributions of tsunami wave height. Furthermore, we obtain a joint distribution of damage probabilities by applying the tsunami damage function.

The outline of the response surface method and copula modeling used in this study is explained below. The response surface method is a statistical combination method to determine an optimum solution using the least number of measurement data possible. The basic idea is based on a reliability-based design scheme developed in the research field of geomechanics (e.g. Honjo, 2011). Generally, the response surface model is given by Eq. (1) as follows:

$$y = f(x_1, x_2, \ldots, x_n) + \varepsilon \tag{1}$$

where explanatory variables correspond to x_i (i = 1, 2, 3, ..., n), response (object variable) corresponds to y, and error corresponds to ε. In this study, we model tsunami wave height with Eq. (2) by following the tsunami hazard evaluation method proposed by Kotani et al. (2016) that applied a reliability analysis framework using the response surface method proposed in Honjo (2011). The expression is as follows:

$$h(S, D) = aS + bD + cSD + dS^2 + e \tag{2}$$

where $h(S, D)$ denotes the tsunami wave height, S denotes the slip ratio, D denotes the fault depth, and a, b, c, d, and e denote the coefficients. This response surface method has an advantage that the probability distribution of the objective variable can be easily evaluated by applying an appropriate probability distribution to the explanatory variable and performing Monte-Carlo simulation. Although tsunami numerical simulation considering uncertainty usually has high calculation cost to conduct vast numbers of simulation cases, it is possible to significantly reduce the simulation cost by using the response surface method.

The foundation of the copula theory corresponds to the Sklar theorem (Sklar, 1959). A copula is a multivariate distribution whose marginals are all uniform over [0, 1]. Given this in combination with the fact that any continuous random variable can be transformed to be uniform over [0, 1] by its probability integral transformation, copulas are used to separately provide multivariate dependence structure from the marginal distributions. Let F be a n-dimensional distribution function with marginals $F_1, \ldots, F_n$ and H be a joint cumulative distribution function. There exists a n-dimensional copula C such that for all x in the domain of F, the following expression holds (Sklar, 1959):

$$H(x_1, \ldots, x_n) = C\{F_1(x_1), \ldots, F_n(x_n)\} = C(u_1, \ldots, u_n),\ u_1, \ldots, u_n \in [0,1] \tag{3}$$

Joe (1997) and Nelsen (1999) proposed the two comprehensive treatments on the topic. The two most common elliptical copulas correspond to the Gaussian copula and the t-copula whose copula functions in the bivariate case correspond to Eqs. (4) and (5).

$$C(u_1, u_2) = \Phi_\Sigma(\Phi^{-1}(u_1), \Phi^{-1}(u_2)) \tag{4}$$

$$C(u_1, u_2) = t_{\Sigma,\nu}(t_\nu{}^{-1}(u_1), t_\nu{}^{-1}(u_2)) \tag{5}$$

The Gaussian copula is simply derived from a multivariate Gaussian distribution function Φ_Σ with mean zero and correlation matrix Σ by transforming the marginals by the inverse of the standard normal distribution function Φ. The t-copula is derived in the same way as the Gaussian copula. Given a multivariate centered t-distribution function $t_{\Sigma,\nu}$ with correlation matrix Σ,

https://doi.org/10.5194/nhess-2019-139
Preprint. Discussion started: 27 May 2019

Natural Hazards and Earth System Sciences Discussions

ν degrees of freedom and with marginal distribution function t_ν. The Archimedean copula is a widely-used copula family. The Archimedean copulas include the Gumbel, Frank, and Clayton copulas whose copula functions in the bivariate case correspond to Eqs. (6), (7), and (8), respectively, as follows:

$$C_\theta(u_1, u_2) = exp\{-[(-lnu_1)^\theta + (-lnu_2)^\theta +]^{1/\theta}\},\ \theta \geq 1 \quad (6)$$

$$C_\theta(u_1, u_2) = -\frac{1}{\theta} ln\left\{1 + \frac{(exp(-\theta u_1)-1)(exp(-\theta u_2)-1)}{exp(-\theta)-1}\right\},\ -\infty < \theta < \infty \quad (7)$$

$$C_\theta(u_1, u_2) = (u_1^{-\theta} + u_2^{-\theta} - 1)^{-1/\theta},\ \theta \geq 1 \quad (8)$$

The Gumbel and Clayton copulas capture upper tail dependence and lower tail dependence, respectively, while the Frank copula does not exhibit tail dependence. Specifically, θ is estimated based on the maximum log-likelihood method. The copulas denote the symmetrical property with respect to diagonal lines of a unit square. To handle asymmetrical data in transformed space, we used an asymmetrical extreme-value copula (Tawn, 1988; Genest and Favre 2007; Genest and Segers, 2009). Extreme-value copulas are characterized by the dependence function *A* as given in Eq. (9):

$$C(u_1, u_2) = exp\left[log(u_1 u_2) A\left\{\frac{log(u_1)}{log(u_1 u_2)}\right\}\right] \quad (9)$$

An asymmetric model using the copula with three parameters as mentioned by Tawn (1988) is given by:

$$A(t) = \{\theta^r (1-t)^r + \varphi^r t^r\}^{1/r} + (\theta - \varphi)t + 1 - \theta \quad (10)$$

where, *r*, θ *and* φ are estimated based on the maximum log-likelihood method. The special case $\theta = 1$ and $\varphi = 1$ corresponds to the symmetric model proposed by Gumbel (1960), and thus this is termed as the asymmetric Gumbel copula. We use this copula for modeling asymmetrical data dependence.

In this study, we use bivariate as the tsunami wave height at two target points and model the correlation using copula. The linear correlation coefficient (Pearson's correlation coefficient) is an index that captures the linear relation between variables and essentially cannot express the dependency between variables that are not in linear relation. Conversely, the copula is a function that expresses the correlation based on the order of the data of each variable rather than the data itself. The order of the data is expressed by Kendall's τ (Kendall, 1938). Therefore, it is possible to quantify the nonlinear correlation between the variables. Table 1 shows theoretical value of Kendall's τ corresponding to the bivariate copulas and their parameter vectors. In this study, we show a simple evaluation method for two target points, although correlation between more points can be considered by using copulas.

3 Application to the Sagami trough area

In this chapter, we demonstrate a case study where the risk assessment method described in the previous chapter is applied for two buildings located on the coast of Sagami Bay, Kanagawa prefecture in Japan. Section 3.1 shows the assessment target points, Section 3.2 shows the tsunami numerical simulation considering uncertainties, Section 3.3 constructs the response surface, Section 3.4 shows the modeling of tsunami wave height correlation using copulas, and Section 3.5 shows the results of the evaluation and discussion.

https://doi.org/10.5194/nhess-2019-139
Preprint. Discussion started: 27 May 2019

Natural Hazards and Earth System Sciences Discussions

3.1 Risk assessment targets

Figure 2 shows the located points of tsunami risk assessment targets, namely Oiso and Miura, Kanagawa prefecture in Japan. Oiso is located at the approximate center of Sagami Bay coast, and Miura is located at the tip of the Miura Peninsula, which is located between Tokyo Bay and Sagami Bay. We assume a steel-framed building located at these two points and evaluate tsunami damage probability for the two buildings.

3.2 Tsunami numerical simulation considering uncertainties

In this section, we evaluate the tsunami wave heights by considering the uncertainty at the target points.

We selected ten earthquake occurrence sources of the Moment magnitude (Mw) 8 class along the Sagami trough announced by NIED (2017), which significantly affects the metropolitan area in Japan. The Sagami trough is a 300 km long boundary between the Philippine Sea and North American plates. The assumed earthquake sources are shown in Fig. 3 (a). The Mw of the sources ranges from Mw 7.9 to Mw 8.6. The region 8 has maximum Mw 8.6. The sources are used for probabilistic ground motion prediction published by NIED (2017), and thus they exhibit 0.7 % occurrence probability in the next 30 years, and the weights of occurrence probability for each earthquake source. We set fault parameters (i.e., slip amount, depth, dip, rake and strike) to the sources based on information published by Cabinet Office (2013) in Japan. Table 2 shows the number of small faults in each source. Each small fault corresponded to a 2.5 km square, and the slip amount of the fault was set to a uniform value based on the moment magnitude (Mw) by using the scaling law of the earthquake. In this study, we did not consider non-uniform slip distribution for purposes of simplicity. Figure 3 (b) shows the calculation results of the initial water level distribution of the tsunami using the Okada (1985) equation. The initial water level of up to about +3.5 m is distributed off to Sagami Bay and Tokyo Bay. Using the initial water level as an input value, we performed a tsunami numerical simulation via a nonlinear long wave equation. We use the following continuity equation (Eq. (11)) and nonlinear shallow water equations (Eqs. (12) and (13)) as follows:

$$\frac{\partial \eta}{\partial t} + \frac{\partial M}{\partial x} + \frac{\partial N}{\partial y} = 0 \tag{11}$$

$$\frac{\partial M}{\partial t} + \frac{\partial}{\partial x}\left[\frac{M^2}{D}\right] + \frac{\partial}{\partial y}\left[\frac{MN}{D}\right] + gD\frac{\partial \eta}{\partial x} + \frac{gn^2}{D^{7/3}}M\sqrt{M^2+N^2} = 0 \tag{12}$$

$$\frac{\partial N}{\partial t} + \frac{\partial}{\partial x}\left[\frac{MN}{D}\right] + \frac{\partial}{\partial y}\left[\frac{N^2}{D}\right] + gD\frac{\partial \eta}{\partial y} + \frac{gn^2}{D^{7/3}}N\sqrt{M^2+N^2} = 0 \tag{13}$$

where η denotes the water level, D denotes the total water level, g denotes the acceleration due to gravity, n denotes the Manning coefficient, and M and N denote the fluxes in the x and y directions, respectively. The governing equations were discretized via the staggered leapfrog scheme (Goto and Ogawa, 1982; UNESCO, 1997). To consider wave height uncertainty, we implemented 25 cases of tsunami numerical simulation for each earthquake source. In each source, the slip amount was varied by ± 0.1 times, ± 0.05 times with respect to the reference case (5 cases) in terms of Mw conversion based on the scaling law, and the fault depth was changed by + 2.0 km, +1.0 km, - 0.5 km, and - 1.0 km with respect to the reference case (5 cases) to consider the changes of the slip and the fault depth as uncertainty. There are a total of 10

https://doi.org/10.5194/nhess-2019-139
Preprint. Discussion started: 27 May 2019


Natural Hazards and Earth System Sciences Discussions

earthquake sources thus, we implemented a total of 250 cases of tsunami numerical simulation nested in four stages of 270 m, 90 m, 30 m, and 10 m in the Japanese plane rectangular coordinate system IX for each simulation and executed the simulation for 3 hours from the earthquake occurrence. Figure 4 shows the maximum tsunami wave heights of Miura and Oiso and Pearson's correlation coefficient relative to the tsunami numerical simulation results of each earthquake source. We confirmed that the correlation coefficient corresponded to at least 0.8 in any region, thus the correlation between tsunami wave height of Miura and Oiso was relatively high. The results suggest that we should evaluate tsunami risk assessment considering the spatial correlation of tsunami wave height between the target points.

3.3 Construction of response surface

In this section, we construct a response surface.

With respect to the results of the maximum wave height of the tsunami numerical simulation, we regressed the response surface (Eq. (2)) using the least squares method. The explanatory variables correspond to the fault slip and the fault depth, and the objective variable denotes the maximum wave height at the target sites. We performed the regression analysis based on all combinations of four explanatory variables ($2^4 - 1 = 15$ cases) and adopted a response surface with a high coefficient of determination and the smallest Akaike Information Criterion (Akaike, 1974). Table 3 shows the AIC values of 15 case regression analyses for Miura and Oiso, and Table 4 shows the regression coefficients of the response surface where AIC corresponds to the minimum in each earthquake source. For example, Fig. 5 (a) (b) shows the response surface for the earthquake source region 8 (Mw: 8.6) with the highest Mw. The blue circle denotes the maximum wave height obtained from the tsunami numerical simulations, and the red curved surface denotes the response surface. The response surfaces accurately represented the results of the tsunami numerical simulation. The response surfaces are in accordance with Eq. (14) (Oiso) and Eq. (15) (Miura) as follows:

$$h(S,D) = 0.6567S + 0.0459D - 0.5189S^2 + 0.5147 \quad (14)$$

$$h(S,D) = 11.1136S - 4.0165S^2 - 3.1327 \quad (15)$$

We can obtain the frequency distribution of the tsunami wave height by giving a probability distribution function that expresses the uncertainty to the explanatory variable (slip ratio S and fault depth D) of the evaluated response surface and performing a Monte-Carlo simulation.

As reported by JSCE (2002), the estimated variation of Mw of an earthquake of the same magnitude is approximately 0.1. Based on the aforementioned value, we set a normal distribution with an average value of 1.0 and a standard deviation of 0.1 for the slip rate by using the scaling law. With respect to the uncertainty of the fault depth, we also set a normal distribution. The average value was set to 0.0 m, and the standard deviation was set to a random number generated from a log normal distribution that was obtained from the seismic observation error data from October 2016 to September 2017 (N = 305,030) as published by the Japan Meteorological Agency (2017). We used the lognormal distribution with an average of 0.12 km and a standard deviation of 0.65 km. We would like to note that it is necessary essentially to apply a probability distribution that appropriately expresses all possible uncertainty to the explanatory variables of the response surface, but in this study we

https://doi.org/10.5194/nhess-2019-139
Preprint. Discussion started: 27 May 2019


Natural Hazards and Earth System Sciences Discussions

applied a relatively limited probability distribution as uncertainty since we did not focus on discussing the details of the tsunami wave uncertainty, but on proposed tsunami risk assessment method using response surface and copulas. Figure 6 (a) (b) shows the frequency distribution of the tsunami wave height obtained by the aforementioned procedure. By using the response surface method, we can significantly reduce the simulation costs for probabilistic tsunami hazard assessment considering uncertainty.

To ascertain the normality of the frequency distributions, we performed the Kolmogorov–Smirnov test. Table 5 shows the results of p-values for each source region. In several cases the p-values were less than 0.05, thereby indicating that the normality of the frequency distribution of the tsunami height is not secured.

3.4 Dependence modelling using copulas

In this section, we estimate appropriate copulas from the results of tsunami numerical simulation considering uncertainties and evaluate spatial correlation structure of tsunami wave height between two sites.

As confirmed in the previous section, despite the high linear correlation of the frequency distribution of the tsunami wave height in Miura and Oiso, it is observed that the normality of tsunami wave height for several sources was not secured by the normality test. The Pearson's correlation coefficient did not accurately grasp the spatial correlation structure of tsunami wave height, and thus we attempt modeling using copula. Hereafter, we only illustrate the analysis results of the earthquake source region 8 (Mw: 8.6) with the largest Mw as an example.

Table 6 shows the results of estimating copulas by maximum likelihood estimation for the distribution obtained via converting the numerical simulation results into [0-1] space. We considered that a copula associated with the smallest AIC (Akaike, 1974) and BIC (Schwarz, 1978) as the best-fit copula. In source region 8, the copula with the smallest AIC and BIC corresponded to the Frank copula. We derived the simultaneous distribution of the tsunami wave heights considering the wave height correlation using the Frank copula and the empirical cumulative distributions obtained from the histogram of the tsunami wave height evaluated in the previous section. Figure 7 shows the Frank copula in [0-1] space, Fig. 8 (a) and (b) shows the empirical cumulative distributions of tsunami wave height for Oiso and Miura, Fig. 9 (a) shows the results considering the wave height correlation and Fig. 9 (b) shows the results without considering the wave height correlation. The black points denote the results of Monte-Carlo simulation. The number of simulations is 10,000. The red points denote the results of tsunami numerical simulation by nonlinear long wave equation. By considering the spatial correlation of the tsunami wave heights using copula, we performed a Monte-Carlo simulation that appropriately captures the nonlinear spatial correlation of the tsunami wave height. We clearly showed the usefulness of copula modeling considering the wave height correlation.

Table 7 shows the result of estimating copulas under the same procedure for other earthquake source regions. In the earthquake source regions targeted in this study, four types of copula were estimated, namely rotated Gumbel copula, asymmetric Gumbel copula, Frank copula, and Gumbel copula. Rotated Gumbel copula corresponds to a copula that rotates the ordinary Gumbel copula by 180 degrees. For reference purposes, the copulas for all earthquake source regions are

https://doi.org/10.5194/nhess-2019-139
Preprint. Discussion started: 27 May 2019


Natural Hazards and Earth System Sciences Discussions

illustrated in Fig. 10. From the characteristics of the copula mentioned before, there is a tail dependency in the wave heights due to the region 1, 2, 3, 5, 7 and 9, but there is no tail dependency in the wave heights due to the region 4, 6, 8 and 10. The tail dependency of the wave height could change in various ways under the effects from the relative position of the earthquake sources and the target points, the bottom and land topography.

3.5 Risk assessment results and discussion

In this section, we evaluate the simultaneous distribution of tsunami wave heights and damage probability of target buildings for the entire area of the Sagami trough earthquake using the occurrence probability weights of each earthquake source.

Table 8 shows the occurrence probability weights of each region of the Sagami trough published by NIED (2017). We first determine the earthquake occurrence region via uniform random numbers using the weights and then evaluate the simultaneous distribution of the tsunami wave heights due to the determined earthquake using the estimated copula. Figure 11 shows the results of evaluation by Monte-Carlo simulation with 10,000 trials. Figure 11 (a) shows the simultaneous distribution of the tsunami wave heights considering the spatial correlation of the wave height, and Fig. 11 (b) shows the results without considering spatial correlation of the tsunami wave height. Furthermore, Fig. 11 (c) shows the simultaneous damage probability of two buildings that transform both axes of tsunami wave heights in Fig. 11 (b) into the damage probability by using the damage function of the steel frame (Suppasri et al., 2013) based on the assumption that a steel building exists at the evaluation target point. Table 9 shows the average value of aggregate damage probability of two buildings, 95 percentile value, 99 percentile value, and maximum value assuming that the two buildings exhibit the same asset value. Although the expected value of the aggregate damage probability barely changed when compared with that of no correlation case, the aggregate damage probability of the ninety-ninth percentile value was approximately 1.0 % higher and the maximum value was approximately 3.0 % higher when considering the hazard correlation utilizing the copulas. We clearly showed the significance of considering spatial correlation structure of tsunami wave height in evaluating tsunami risks for a portfolio of buildings. In this study we only demonstrated the evaluation method for two points, but the effect of the wave height correlation on the evaluation result is expected to increase if more points are targeted.

4 Conclusion

In this study, we evaluated the aggregate tsunami damage probability of two buildings located at two relatively remote locations based on the frequency distribution of the tsunami height via the response surface method and the spatial correlation of the tsunami height by using various copulas, assuming the occurrence of the Sagami Trough earthquake that significantly affects the metropolitan area in Japan. The ninety-ninth percentile value of the aggregate damage probability was approximately 1.0 % higher, and the maximum value was approximately 3.0 % higher in the evaluation considering the spatial correlation of the tsunami wave height when compared with the evaluation without considering the spatial correlation. The results clearly show the significance of considering the spatial correlation of the tsunami hazard in evaluating tsunami

https://doi.org/10.5194/nhess-2019-139
Preprint. Discussion started: 27 May 2019


Natural Hazards and Earth System Sciences Discussions

risks for a building portfolio and suggest that spatial correlation modeling by copulas is effective in the case wherein nonlinear correlation of the hazard exists. In addition, the response surface method used in this study significantly reduces the simulation costs for probabilistic tsunami hazard assessment considering uncertainty. It is expected that the tsunami risk assessment method for a portfolio of buildings over a wide area as proposed in this study can be used for probabilistic tsunami risk assessment of real estate portfolios or business continuity plans by parties such as large companies, insurance companies and real-estate agency.

Acknowledgement

We thank anonymous reviewers who provided us valuable comments and helped improve the manuscript. This research was partially supported by funding from the International Research Institute of Disaster Science (IRIDeS) at Tohoku University.

References

Akaike, H.: A new look at the statistical model identification, IEEE Trans Automatic Control, 19(6), 716–723, doi:10.1109/TAC.1974.1100705, 1974.

Annaka, T., Satake, K., Sakakiyama, T., Yanagisawa, K., and Shuto, N.: Logic-tree Approach for Probabilistic Tsunami Hazard Analysis and its Applications to the Japanese Coasts, Pure Appl. Geophys., 164, 577–592, doi:10.1007/s00024-006-0174-3, 2007.

Boore, D. M., Gibbs, J. F., Joyner, W. B., Tinsley, J. C., and Ponti, D. J.: Estimated ground motion from the 1994 Northridge, California, earthquake at the site of the interstate 10 and La Cienega Boulevard bridge collapse, West Los Angeles, California, Bull. Seism. Soc. Amer., 93(6), 2737–2751, doi:10.1785/0120020197, 2003.

Cabinet Office, The study meeting for the Tokyo Inland Earthquakes, http://www.bousai.go.jp/kaigirep/chuobou/senmon/shutochokkajishinmodel/, last access: 11 May 2018, 2013.

Fukutani, Y., Suppasri, A., and Imamura, F.: Stochastic analysis and uncertainty assessment of tsunami wave height using a random source parameter model that targets a Tohoku-type earthquake fault, Stoch. Environ. Res. Risk. Assess., 29, 1763–1779, doi:10.1007/s00477-014-0966-4, 2015.

Geist, E. L., and Parsons, T.: Probabilistic analysis of tsunami hazards, Nat. Hazards., 37, 277–314, doi:10.1007/s11069-005-4646-z, 2006.

Genest, C., and Favre, A. C.: Everything You Always Wanted to Know about Copula Modeling but Were Afraid to Ask, J. Hydro. Eng., 12(4), 347–368, doi:10.1061/(ASCE)1084-0699(2007)12:4(347), 2007.

Genest, C., and Segers, J.: RANK-BASED INFERENCE FOR BIVARIATE EXTREME-VALUE COPULAS, Annals of Statistics, 37(5B), 2990–3022, doi:10.1214/08-AOS672, 2009.

https://doi.org/10.5194/nhess-2019-139
Preprint. Discussion started: 27 May 2019

Goda, K., Mai, P. M., Yasuda, T., and Mori, N.: Sensitivity of tsunami wave profiles and inundation simulations to earthquake slip and fault geometry for the 2011 Tohoku earthquake, Earth Planets Space, 66, 105, doi:10.1186/1880-5981-66-105, 2014.

Goda, K., and Tesfamariam, S.: Multi-variate seismic demand modelling using copulas: Application to non-ductile reinforced concrete frame in Victoria, Canada, Structural Safety, 56, 39–51. doi:10.1016/j.strusafe.2015.05.004, 2015.

González, F. I., Geist, E. L., Jaffe, B., Kânoğlu, U., Mofjeld, H., Synolakis, C. E., Titov, V. V., Arcas, D., Bellomo, D., and Carlton, D.: Probabilistic tsunami hazard assessment at seaside, Oregon, for near and far field seismic sources, J. Geophys. Res. Oceans., 114, C11023, doi:10.1029/2008JC005132, 2009.

Goto, C., and Ogawa, Y.: Tsunami numerical simulation with Leap-frog scheme, Tohoku University, 52p, 1982.

Gumbel, E. J.: Distributions des valeurs extrˆemes en plusieurs dimensions, Publ. Inst. Statist. Univ. Paris, 9, 171–173, MR0119279, 1960.

Honjo, Y.: Challenges in geotechnical reliability based design, Proceedings of 3rd International Symposium on Geotechnical Safety and Risk, 11–27, 2011.

Joe, H.: Multivariate Models and Dependence Concepts, Chapman & Hall Ltd, 424p, 1997.

Japan Society of Civil Engineers: Tsunami Assessment Method for Nuclear Power Plants in Japan., http://committees.jsce.or.jp/ceofnp/node/5, last access: 30 August 2015, 2002.

Japan Meteorological Agency: Centralized processing earthquake source lists, 2017. https://hinetwww11.bosai.go.jp/auth/?LANG=ja, last access: 11 May 2018, 2017.

Kendall, M.: A New Measure of Rank Correlation, Biometrika, 30(1-2), 81–93, doi:10.1093/biomet/30.1-2.81, 1938.

Kotani, T., Takase, S., Moriguchi, S., Terada, K., Fukutani, Y., Otake, Yu., Nojima, K., and Sakuraba, M.: NUMERICAL-ANALYSIS-AIDED PROBABILISTIC TSUNAMI HAZARD EVALUATION USING RESPONSE SURFACE, J. Japan Soc. Civil. Eng., Ser. A2 (Applied Mechanics (AM)) 72(1), 58–69, doi:10.2208/jscejam.72.58, 2016.

Løvholt, F., Pedersen, G., Bazin, S., Kuhn, D., Bredesen, R. E., and Harbitz, C.: Stochastic analysis of tsunami runup due to heterogeneous coseismic slip and dispersion, J. Geophys. Res., 117, C03047, doi:10.1029/2011JC007616, 2012.

NIED (National Research Institute for Earth Science and Disaster Resilience): Japan Seismic Hazard Information Station, http://www.j-shis.bosai.go.jp/map/, last access: 11 May 2018, 2017.

Nelsen, R. B.: An Introduction to Copulas. Springer-Verlag, 199p, 1999.

Okada, Y.: Surface deformation due to shear and tensile faults in a half-space, Bull. Seism. Soc. Amer., 75(4), 1135–1154, 1985.

Park, H., and Cox, D. T.: Probabilistic assessment of near-field tsunami hazards: Inundation depth, velocity, momentum flux, arrival time, and duration applied to Seaside, Oregon, Coast. Eng., 117, 79–96, doi:10.1016/j.coastaleng.2016.07.011, 2016.

https://doi.org/10.5194/nhess-2019-139
Preprint. Discussion started: 27 May 2019

Park, J., Bazzurro, P., and Baker, J. W.: Modeling spatial correlation of ground motion intensity measures for regional seismic hazard and portfolio loss estimation, Tenth International Conference on Application of Statistic and Probability in Civil Engineering (ICASP10), Tokyo, Japan, 2007.

Raffaele, D. R., and Goda, K.: Probabilistic Earthquake-tsunami Hazard Assessment: The First Step Towards Resilient Coastal Communities, Procedia Engineering, 198, 1058–1069, doi:10.1016/j.proeng.2017.07.150, 2017.

Salvadori, G., Durante, F., Michele, C. D., Bernardi, M., and Petrella, L.: A multivariate copula-based framework for dealing with hazard scenarios and failure probabilities, Water Resour. Res., 52, 3701–3721, doi:10.1002/2015WR017225, 2016.

Schwarz, G. E.: Estimating the dimension of a model, Annals of Statistics, 6(2), 461–464, 1978.

Sklar A. W.: Fonctions de r´epartition `a n dimension et leurs marges, Publications de l'Institut de Statistique de l'Universit´e de Paris, 8, 229–231, 1959.

Suppasri, A., Mas, E., Charvet, I., Gunasekera, R., Imai, K., Fukutani, Y., Abe, Y., and Imamura, F.: Building damage characteristics based on surveyed data and fragility curves of the 2011 Great East Japan tsunami, Nat. Hazards, 66, 319–341. doi:10.1007/s11069-012-0487-8, 2013.

Tawn, J. A.: Bivariate extreme value theory: Models and estimation, Biometrika, 75(3), 397–415, doi:10.2307/2336591, 1988.

Thio, H. K., Somerville, P. G., and Polet, J.: Probabilistic Tsunami Hazard in California. College of Engineering, University of California: Los Angeles, CA, USA, 2010.

UNESCO, IUGG/IOC Time Project: Numerical method of tsunami simulation with the leap-flog scheme. IOC Manuals and Guides No. 35, 1997.

Wang, M., and Takada, T.: Macro-spatial correlation model of seismic ground motions, Proceedings of ICOSSAR'05, 353–360, Millpress, Rotterdam, 2005.

https://doi.org/10.5194/nhess-2019-139
Preprint. Discussion started: 27 May 2019

Natural Hazards and Earth System Sciences
Discussions

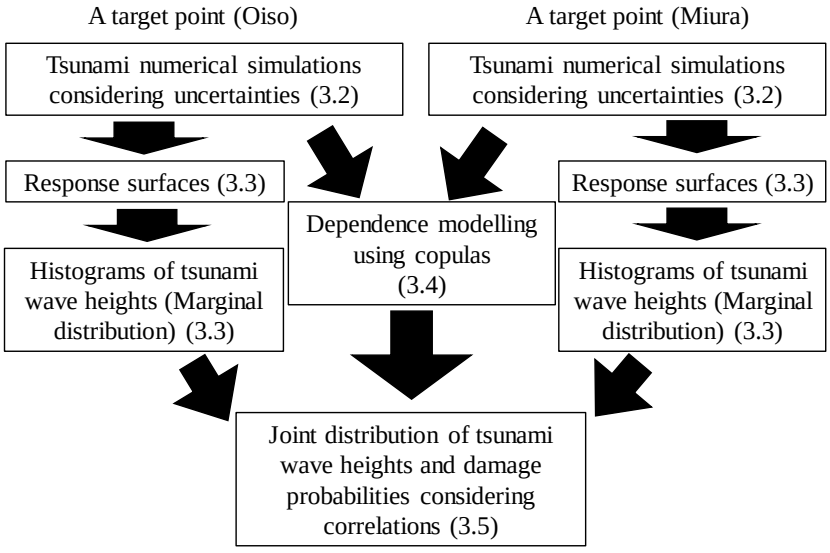

Figure 1: Flowchart of probabilistic tsunami risk assessment considering spatial correlation of tsunami wave height. Numbers in the parentheses indicate the section numbers escribed.

5

Table 1: Bivariate copula, parameter vectors, Kendall's tau

Copula	Parameter vectors	Kendall's tau
Gaussian copula	ρ	$(2/\pi)\arcsin\rho$
t copula	ρ, ν	$(2/\pi)\arcsin\rho$
Clayton copula	θ	$\theta/(\theta+2)$
Frank copula	θ	$1-4/\theta+4D_1(\theta)/\theta$
Gumbel copula	θ	$1-1/\theta$
Asymmetric Gumbel copula	r, θ, φ	$\int_0^1 \frac{t(1-t)A''(t)}{A(t)}dt$

10 **ρ: Pearson's correlation coefficient, $D_1(\theta) = \int_0^\theta \frac{\frac{x}{\theta}}{(e^x-1)}dx$: the first Debye function**

https://doi.org/10.5194/nhess-2019-139
Preprint. Discussion started: 27 May 2019

Natural Hazards and Earth System Sciences
Discussions

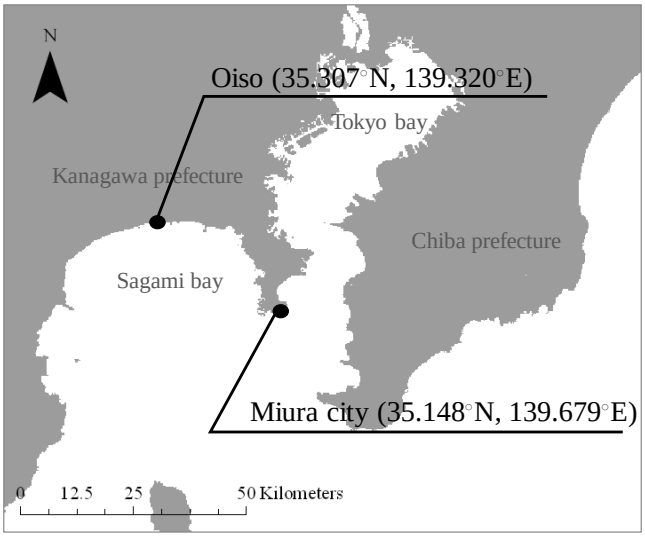

Figure 2: Two targets points, Oiso and Miura in Kanagawa prefecture for tsunami risk assessment

Table 2: Source region of the Sagami trough earthquake, Moment magnitude, Average slip and Number of faults in each earthquake source

Source region number	Moment magnitude (Mw)	Average slip (m)	Number of faults
1	7.9	2.5	1207
2	8.2	4.0	2392
3	8.0	2.7	1533
4	8.3	4.6	3393
5	8.4	5.0	3599
6	8.5	5.8	4926
7	8.5	5.2	4822
8	8.6	6.3	6149
9	7.9	2.5	1234
10	8.2	3.0	2825

https://doi.org/10.5194/nhess-2019-139
Preprint. Discussion started: 27 May 2019

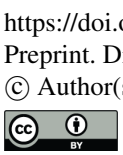

Natural Hazards and Earth System Sciences
Discussions

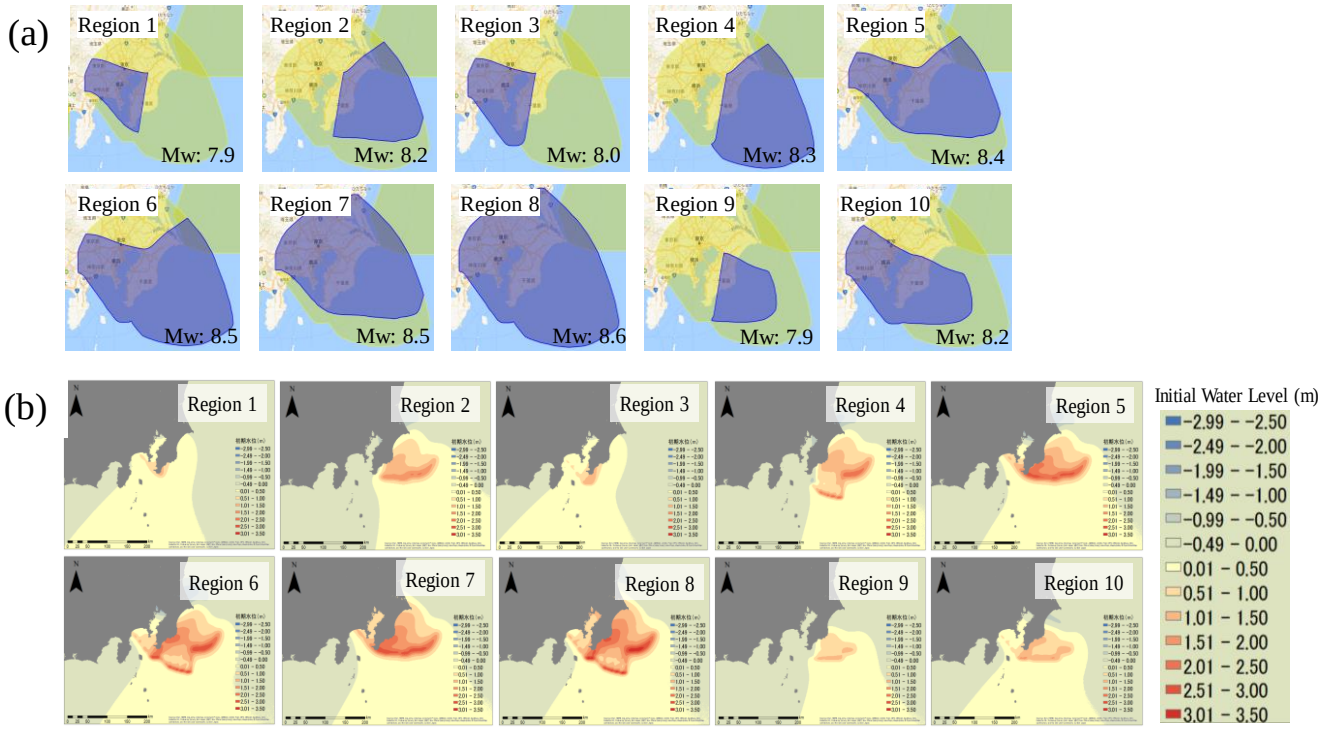

Figure 3: (a) The Sagami trough earthquakes of ten regions (NIED, 2017) and (b) Initial water levels of tsunami calculated from the fault parameters using Okada equation. (Okada, 1985)

5

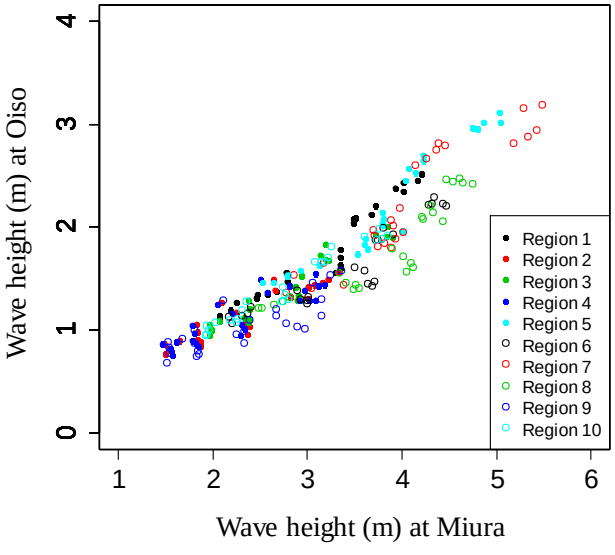

	Pearson's correlation coefficient
Region 1	0.99
Region 2	0.90
Region 3	0.95
Region 4	0.88
Region 5	0.98
Region 6	0.96
Region 7	0.95
Region 8	0.95
Region 9	0.81
Region 10	0.99

Figure 4: Maximum tsunami wave heights simulated from tsunami numerical simulation at Miura and Oiso and Pearson's correlation coefficients in each region.

https://doi.org/10.5194/nhess-2019-139
Preprint. Discussion started: 27 May 2019

Natural Hazards and Earth System Sciences
Discussions

Table 3: Akaike Information Criterion (AIC) results of the regression analyses.

The regression analysis were performed based on all combinations of four explanatory variables.

Oiso	Cases of the response surface															
	1	2	3	4	5	6	7	8	9	10	11	12	13	14	15	Minimum
Region 1	-86.1073	-75.0959	-76.4418	-86.0675	-83.3907	-69.8912	-47.8628	-83.6900	37.3278	-76.0403	-75.3817	-46.9466	-48.9226	36.8890	36.3744	-86.1073
Region 2	-70.4205	-62.1961	-66.0866	-71.2517	-71.4697	-60.0875	-47.2552	-72.3436	8.2820	-63.5425	-67.3455	-45.3779	-48.9304	7.5681	6.9034	-72.3436
Region 3	-78.1960	-69.4144	-73.0031	-78.9561	-79.9437	-66.8035	-51.6857	-80.7160	24.0401	-70.7359	-74.8137	-50.0483	-53.6110	23.5389	22.9902	-80.7160
Region 4	-70.3635	-62.7432	-67.6975	-72.0181	-71.4781	-61.7123	-46.0815	-73.1446	6.5531	-64.5753	-68.9606	-44.5848	-47.7924	6.0516	5.2790	-73.1446
Region 5	-84.3052	-79.8555	-83.1754	-86.2150	-70.7497	-79.5811	-51.9906	-72.7012	45.9869	-81.7477	-71.0212	-52.3149	-49.3924	45.8946	45.4242	-86.2150
Region 6	-84.3409	-85.3398	-81.8169	-85.7067	-71.5073	-83.0709	-64.9049	-73.1549	31.6107	-86.7700	-70.9075	-66.5245	-60.0166	31.2625	30.8593	-86.7700
Region 7	-21.7317	-18.3202	-23.5936	-23.7244	-23.6513	-20.2440	-22.2107	-25.6440	48.8843	-20.3017	-25.5136	-19.4355	-24.1409	48.7116	48.3525	-25.6440
Region 8	-81.1962	-79.0259	-77.2264	-82.0455	-73.1696	-76.0809	-59.6378	-74.3933	35.9058	-80.1470	-71.0190	-60.0970	-57.5528	35.5037	35.0967	-82.0455
Region 9	-31.0739	-32.3196	-31.8511	-32.9766	-29.8352	-33.0836	-25.1204	-31.7497	4.7047	-34.2103	-30.7579	-26.6012	-24.8998	3.8330	3.1376	-34.2103
Region 10	-80.2635	-69.9115	-73.6468	-80.1713	-82.1713	-66.6323	-53.8587	-82.0864	23.4459	-70.7917	-75.5814	-51.5993	-55.8313	22.8583	22.3445	-82.1713

Miura	Cases of the response surface															
	1	2	3	4	5	6	7	8	9	10	11	12	13	14	15	Minimum
Region 1	-29.9142	-3.7669	-29.5662	-31.5773	-18.4609	-5.1563	-19.9724	-20.2637	56.8927	-5.7181	-19.0634	-2.3947	-13.4162	56.4377	55.9832	-31.5773
Region 2	-32.4696	-21.1006	-34.4497	-34.1257	-32.7950	-23.1000	-32.9901	-34.4733	51.9175	-22.9686	-34.7765	-23.0689	-33.5269	51.4723	51.5649	-34.7765
Region 3	-43.3459	-30.2321	-43.9870	-43.9721	-44.8801	-31.6225	-45.9601	-45.5310	55.2425	-31.6189	-45.5456	-33.6121	-47.5191	54.6938	54.6028	-47.5191
Region 4	-22.4764	-12.7328	-23.4804	-21.3515	-22.0638	-14.2238	-15.3526	-21.2106	50.6507	-12.9471	-23.1577	-9.3945	-15.7799	49.5413	49.8184	-23.4804
Region 5	-3.5315	1.5932	-4.8179	-5.3684	-4.4497	0.0418	-3.8392	-6.2935	58.8979	-0.3264	-5.7659	0.3814	-4.9032	58.3657	58.0118	-6.2935
Region 6	-16.9265	8.9520	-18.5645	-18.6108	-3.1964	7.0088	-20.5546	-5.0276	61.2059	6.9971	-5.0028	5.0157	-6.9975	60.6742	60.5649	-20.5546
Region 7	3.3372	1.3587	2.1765	1.5142	3.7790	0.1910	3.8906	1.9395	63.6719	-0.4676	2.5413	1.9058	3.9420	63.0994	62.7084	-0.4676
Region 8	-27.0282	19.0202	-27.1925	-26.7027	7.9340	17.1854	-28.3906	6.4835	60.0863	17.2428	6.3645	15.2927	4.5602	59.1621	59.1455	-28.3906
Region 9	-34.2223	-26.1205	-36.1871	-36.0073	-35.9841	-28.1145	-36.7777	-37.7711	52.5198	-28.0294	-37.9493	-29.1978	-38.5528	52.1439	52.1581	-38.5528
Region 10	-55.5283	-42.4949	-53.1771	-54.3099	-57.3486	-42.2671	-54.1155	-56.1518	55.2739	-42.9033	-55.0260	-43.5964	-55.9706	54.6558	54.4912	-57.3486

Table 4: Regression coefficients of selected each response surface for each source region

Oiso	Regression coefficients				
	a	b	c	d	e
Region 1	1.1705	0.1039	-0.0371	0.3051	0.1927
Region 2	0.9868	0.0598	0.0000	0.0000	0.1037
Region 3	1.3747	0.0566	0.0000	0.0000	0.0040
Region 4	0.9568	0.0625	0.0000	0.0000	0.1184
Region 5	0.7991	0.0592	0.0000	0.6449	0.6303
Region 6	0.0000	0.0404	0.0000	0.7610	0.7538
Region 7	2.2360	0.0445	0.0000	0.0000	-0.0971
Region 8	0.6567	0.0459	0.0000	0.5189	0.5147
Region 9	0.0000	0.0661	0.0000	0.3945	0.5739
Region 10	-1.3690	-0.0972	0.0423	0.0000	-0.0029

Miura	Regression coefficients				
	a	b	c	d	e
Region 1	6.2764	0.0832	0.0000	-1.7394	-1.3700
Region 2	2.3946	0.0000	-0.0336	0.0000	-0.1281
Region 3	2.5601	0.0000	0.0000	0.0000	0.2187
Region 4	3.8893	0.0000	-0.0767	-0.7610	-0.8384
Region 5	2.6802	0.0643	0.0000	0.0000	1.0744
Region 6	8.0738	0.0000	0.0000	-2.5004	-2.1023
Region 7	0.0000	0.0829	0.0000	1.3910	2.4982
Region 8	11.1136	0.0000	0.0000	-4.0165	-3.1327
Region 9	2.4222	0.0000	0.0000	0.0000	-0.1673
Region 10	-2.5917	-0.1083	0.0869	0.0000	-0.1061

https://doi.org/10.5194/nhess-2019-139
Preprint. Discussion started: 27 May 2019

Natural Hazards and Earth System Sciences
Discussions

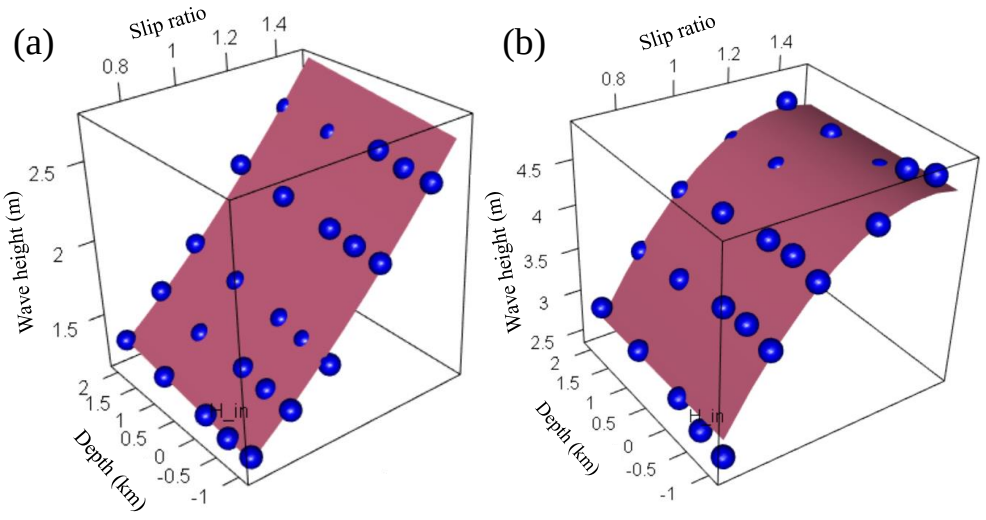

Figure 5: Response surfaces at (a) Oiso and (b) Miura for Region 8 of the Sagami trough. The blue circle denotes the maximum wave height obtained from the tsunami numerical simulations and the red curved surface denotes the response surface.

5

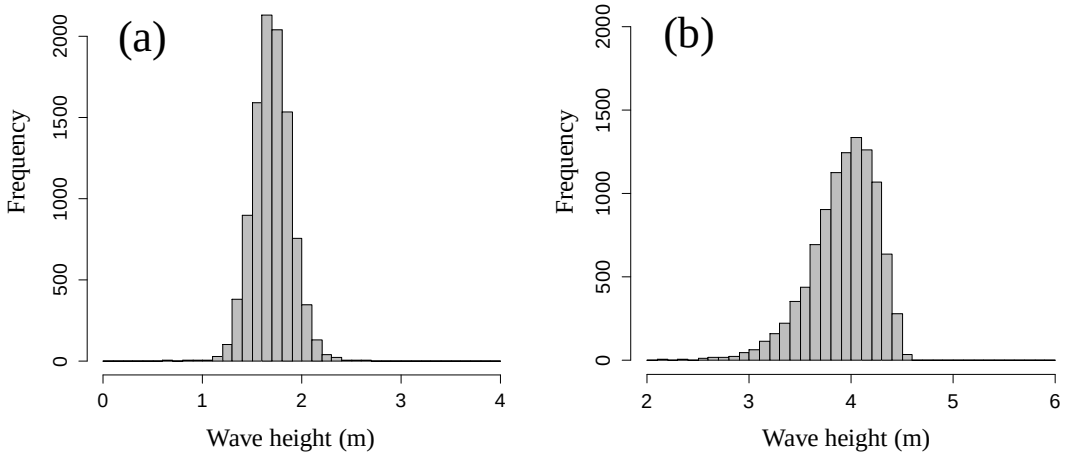

Figure 6: Histograms of tsunami wave height simulated from the response surface at (a) Oiso and (b) Miura for Region 8 of the Sagami trough

https://doi.org/10.5194/nhess-2019-139
Preprint. Discussion started: 27 May 2019

Natural Hazards and Earth System Sciences
Discussions

Table 5: Kolmogorov–Smirnov test results

	p-value	
	Oiso	Miura
Region 1	0.00	0.00
Region 2	0.00	0.89
Region 3	0.00	0.61
Region 4	0.00	0.15
Region 5	0.07	0.95
Region 6	0.72	0.02
Region 7	0.79	0.50
Region 8	0.26	0.00
Region 9	0.00	0.93
Region 10	0.03	0.97

Table 6: Maximum likelihood estimation results of each copulas for Region 8

Name of copulas	Log-likelihood	AIC	BIC
Gaussian copula	24.72	-47.43	-46.21
t-copula	24.62	-45.23	-42.79
Clayton copula	24.46	-46.93	-45.71
Gumbel copula	20.03	-38.06	-36.84
Frank copula	26.16	-50.33	-49.11
rotated Clayton copula	14.53	-27.06	-25.84
rotated Gumbel copula	25.77	-49.54	-48.32
asymmetric Gumbel copula	19.90	-35.80	-33.36
rotated Asymmetric Gumbel copula	25.69	-47.38	-44.94

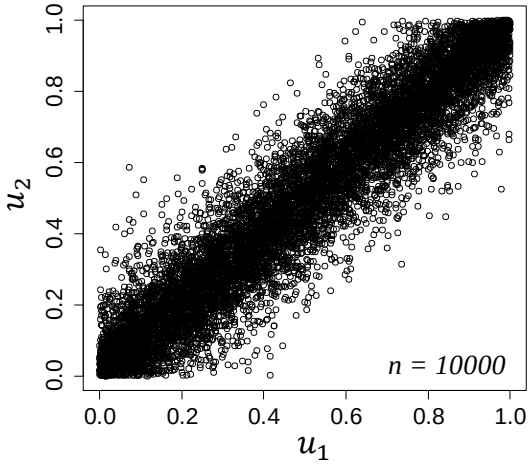

Figure 7: Frank copula for Region 8

https://doi.org/10.5194/nhess-2019-139
Preprint. Discussion started: 27 May 2019

Natural Hazards and Earth System Sciences
Discussions

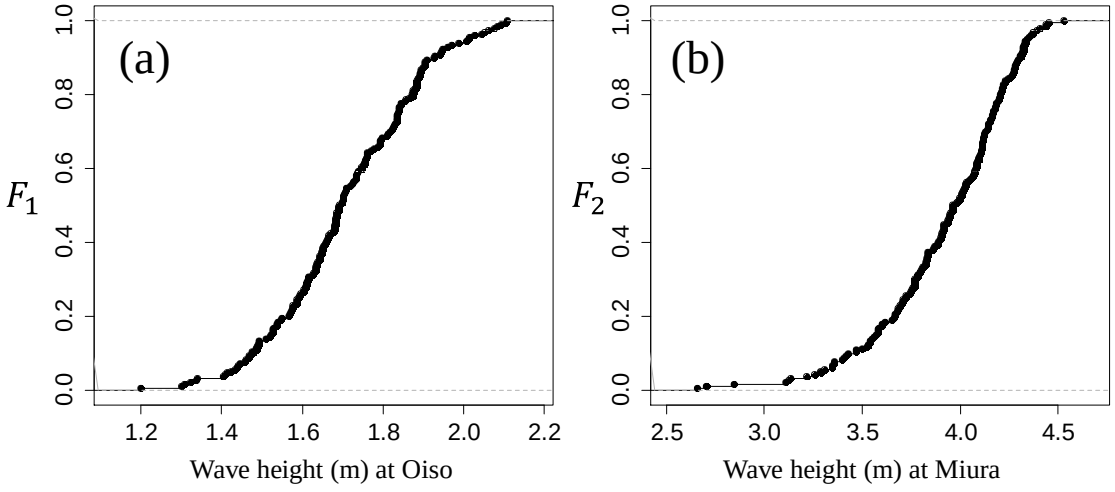

Figure 8: Empirical cumulative distributions of tsunami wave height for (a) Oiso and (b) Miura

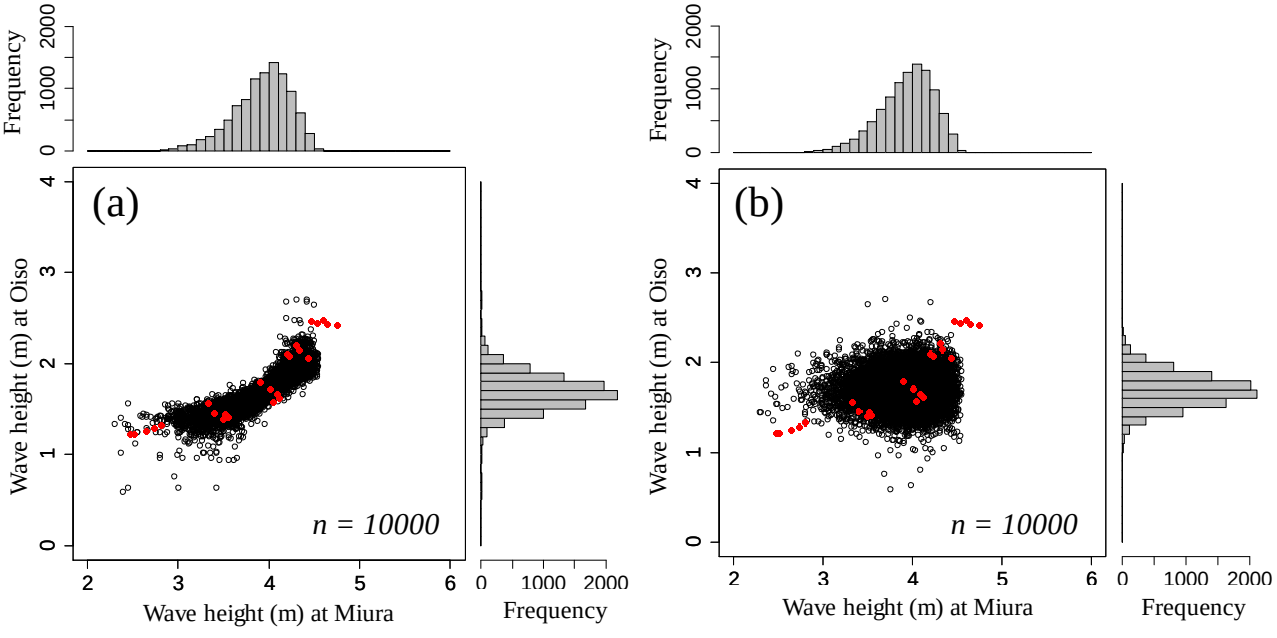

Figure 9: Monte-Carlo simulation results for Region 8. The black points denote the results with 10,000 trials (a) considering and (b) not considering the spatial correlation of tsunami wave heights using the Frank copulas. The red points denote the results calculated from 25 cases of tsunami numerical simulation.

https://doi.org/10.5194/nhess-2019-139
Preprint. Discussion started: 27 May 2019

Natural Hazards and Earth System Sciences
Discussions

Table 7: Estimated optimal copulas, copula parameters, and Kendall's tau for each region of the Sagami trough earthquake

	Estimated copulas	Parameters	Kendall's τ
Region 1	rotated Gumbel copula	20.42	0.95
Region 2	asymmetric Gumbel copula	1.00, 5.08, 0.85	0.70
Region 3	rotated Gumbel copula	4.62	0.78
Region 4	Frank copula	10.54	0.68
Region 5	rotated Gumbel copula	9.24	0.89
Region 6	Frank copula	22.11	0.83
Region 7	Gumbel copula	5.68	0.82
Region 8	Frank copula	17.77	0.80
Region 9	Gumbel copula	2.87	0.65
Region 10	Frank copula	35.76	0.89

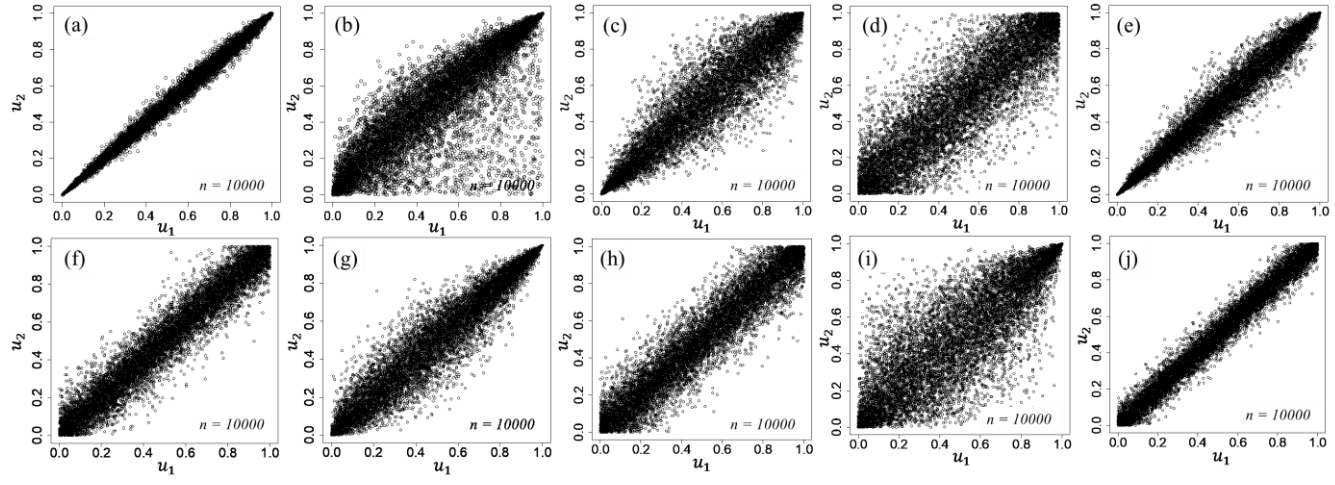

Figure 10: Estimated optimal copulas distributed on $[0, 1]^2$ with 10,000 trials. (a) rotated Gumbel copula for the region 1, (b) asymmetric Gumbel copula for the region 2, (c) rotated Gumbel copula for the region 3, (d) Frank copula for the region 4, (e) rotated Gumbel copula for the region 5, (f) Frank copula for the region 6, (g) Gumbel copula for the region 7, (h) Frank copula for the region 8, (i) Gumbel copula for the region 9, (j) Frank copula for the region 10

https://doi.org/10.5194/nhess-2019-139
Preprint. Discussion started: 27 May 2019

Natural Hazards and Earth System Sciences
Discussions

Table 8: Occurrence probability weights of each region of the Sagami trough (NIED, 2017)

	Occurrence probability weights
Region 1	0.37
Region 2	0.06
Region 3	0.30
Region 4	0.05
Region 5	0.03
Region 6	0.01
Region 7	0.01
Region 8	0.02
Region 9	0.11
Region 10	0.04
Summation	1.00

Table 9: Tsunami risk assessment results

	Aggregate damage probability of two buildings		
	No correlation (A)	Correlation (B)	Difference (B-A)
Average	58.8%	58.8%	0.0%
95 percentile	66.2%	67.0%	0.9%
99 percentile	68.9%	69.7%	0.8%
Maximum	73.5%	76.7%	3.1%

https://doi.org/10.5194/nhess-2019-139
Preprint. Discussion started: 27 May 2019

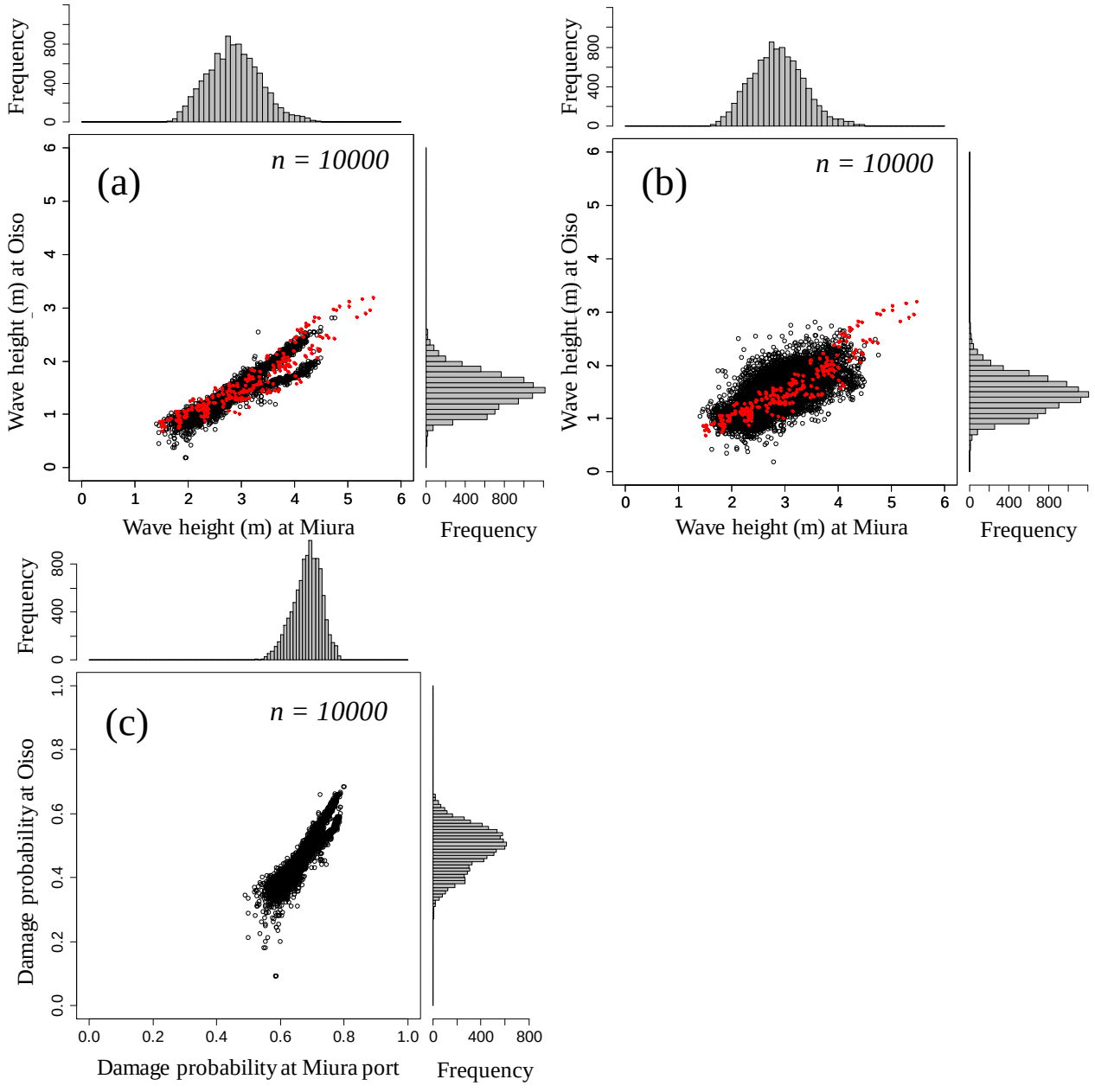

Figure 11: (a) Simultaneous distribution of tsunami wave height considering wave height correlation (b) not considering wave height correlation and (c) Simultaneous damage probability. The black points denote the Monte-Carlo simulation results with 10,000 trials and the red points denote the results simulated via tsunami numerical simulations.